Reduced-Order Stochastic Testing of Interconnects Subject to Line Edge Roughness

Martijn Huynen, Ruben Waeytens, Dries Bosman, Michiel Gossye, Hendrik Rogier and Dries Vande Ginste
quest, Department of Information Technology, Ghent University/imec, Belgium
www.questlab.be
martijn.huynen@ugent.be

***Abstract*—In this contribution we study the propagation constant of interconnects subject to line edge roughness by means of an efficient stochastic framework. By employing the stochastic testing method, we succeed in limiting the number of calls to the full-wave electromagnetic field solver at the core of the system. Additionally, the computationally burdensome solution of the eigenvalue problem is eased by reducing its order through projection on an appropriate basis. The resulting two-step acceleration leads to an effective approach to assess the effect of line edge roughness on the characteristics of interconnects. The novel framework is applied to a rough rectangular waveguide and a microstrip.**

***Index Terms*—interconnects, surface roughness, stochastic testing , reduced order modeling**

I. Introduction

The push towards ever higher frequencies, more compact components and increasing heterogeneous integration raises the complexity in the design of electronic circuits and systems. Physical phenomena that could previously be ignored without detrimental consequences are now more than ever inevitable and should be included in the designer's tools to assess their influence from the get-go. Surface roughness and line edge roughness (LER) [1] are prime illustrations of such phenomena that refer to the non-ideal, irregular profile of conductors. Whether present due to the production process or intentionally applied to obtain cohesion between various layers, its effect on the performance is getting stronger due to miniaturization and a more developed skin effect. Given the random nature of line edge and surface roughness, stochastic methods built around full-wave electromagnetic modeling simulators are the most appropriate tools. However, dealing with the complicated geometry of a coarse surface or edge is a time-consuming effort for full-wave tools, not to mention the numerous runs required for distribution estimation in a stochastic context.

Here, we continue the work outlined in [2], where a set of sparse stochastic methods to capture LER's influence on the propagation constant of a rectangular waveguide was modeled and analyzed. In that paper, the sparse polynomial chaos (SPC) method [3] and a sparse grid version of stochastic testing (ST) [4], [5] are deployed for the waveguide analysis. Both methods strongly reduce the number of calls required to the full-wave solver, which is a finite-element method (FEM) in this study. However, the generalized eigenvalue problem that needs to be solved remains a costly operation that is unavoidable for every single instance of the FEM simulation and it thus is an important bottleneck in the computation cost. Therefore, we propose to modify the model order reduction approach presented in [6] to be applicable to the pertinent eigenvalue problem. This allows for the solution to be sped up considerably without any discernible loss in accuracy. Our improved technique is validated via the analysis of the TE_{10} mode of a rectangular waveguide and comparison with the sparse ST method. Additionally, it is applied to a microstrip configuration.

979-8-3503-3282-7/23/$31.00 ©2023 IEEE

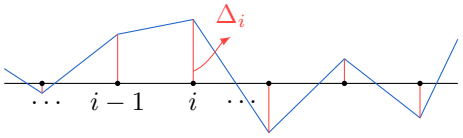

Fig. 1. The line edge roughness (LER) is realized by shifting every ith point on the nominal (black) edge by a random height variation Δ_i perpendicular to the edge.

II. Sparse grid stochastic testing

Consider a 2-D waveguide configuration with the z-axis as the direction of invariance and a $e^{-j\beta z}$ dependence of the modal fields, with β the propagation constant of the mode. Solving the field distribution in the cross-section by means of a pertinent set of hierarchical vector basis functions [7] and testing with a Galerkin approach, results in the following quadratic eigenvalue problem:

$$\left[\overline{\overline{M}}\beta^2 + \overline{\overline{C}}\beta + \overline{\overline{K}}\right]\mathbf{v} = 0. \tag{1}$$

Cast in a generalized eigenvalue form, it can be written as

$$\begin{bmatrix} \overline{\overline{C}} & \overline{\overline{K}} \\ -\overline{\overline{I}} & 0 \end{bmatrix}\begin{bmatrix} \beta\mathbf{v} \\ \mathbf{v} \end{bmatrix} = \beta\begin{bmatrix} -\overline{\overline{M}} & 0 \\ 0 & -\overline{\overline{I}} \end{bmatrix}\begin{bmatrix} \beta\mathbf{v} \\ \mathbf{v} \end{bmatrix} \Leftrightarrow \overline{\overline{A}}\mathbf{x} = \beta\overline{\overline{B}}\mathbf{x}, \tag{2}$$

with $\overline{\overline{I}}$ the identity matrix of size n, i.e., the number of basis functions. Matrices $\overline{\overline{C}}$, $\overline{\overline{K}}$ and $\overline{\overline{M}}$ are easily constructed through the standard derivation of the finite element method. The solution of (2) yields the sought-after propagation constants β of the given waveguide.

As demonstrated in Fig. 1 and similar to the procedure outlined in [8], [9], the rough edges are realized by shifting points $\mathbf{r}_i$ on these lines randomly over a distance Δ_i, which are

random variables (RVs) governed by a multivariate Gaussian distribution. The elements of the accompanying correlation matrix $\overline{\overline{\Sigma}}$ are given by

$$\overline{\overline{\Sigma}}_{ij} = \sigma_r^2 \exp\left(-||\mathbf{r}_i - \mathbf{r}_j||_{\partial\Omega}^2 / L_c^2\right), \tag{3}$$

with $||\cdot||_{\partial\Omega}$ the distance measured along the contour, σ_r the standard deviation of the matrix and L_c the correlation length, i.e., a measure for the dependency on neighboring heights. The correlated set of height variations is subsequently approximated through the Karhunen-Loève transform (KLT) by a (smaller) set of N_{RV} stochastically independent normal random variables $\boldsymbol{\xi}$ tweaked by a threshold parameter Θ (see [2] for more details).

At this point, the sought-after distribution of the propagation constant β is modeled by a polynomial chaos expansion (PCE):

$$\beta(\boldsymbol{\xi}) \approx \sum_{k=0}^{K} a_k \phi_k(\boldsymbol{\xi}), \tag{4}$$

where $K+1$ orthonormal polynomials ϕ_k are employed with unknown expansion coefficient a_k. If all polynomials up to the order P_{max} are included for N_{RV} RVs, the number of polynomials equals

$$K+1 = \frac{(P_{\text{max}} + N_{\text{RV}})!}{P_{\text{max}}!\, N_{\text{RV}}!}. \tag{5}$$

To find the unknowns a_k, stochastic testing [4] is employed, which computes (4) for $K+1$ *interesting* realizations $\boldsymbol{\xi}_i$, resulting in a set of equations:

$$\boldsymbol{\beta} = \overline{\overline{\Phi}} \cdot \mathbf{a} \Leftrightarrow \beta(\boldsymbol{\xi}_i) = \sum_{k=0}^{K} a_k \phi_k(\boldsymbol{\xi}_i) \quad \forall i \in \{0, \ldots, K\}. \tag{6}$$

The crux of the matter now remains to select those points $\boldsymbol{\xi}_i$. In the node picking algorithm [4], a quadrature-based tensor grid is constructed first from which nodes with higher weights are preferentially selected while at the same time orthogonalizing the candidate set to ensure the conditioning of (6). However, the curse of dimensionality cripples ST as well: when applying this method to a problem with a growing number of RVs, which easily occur in LER experiments, the number of required evaluations of the full-wave solver rises fast. Moreover, the node selection process slows down considerably as the next node with the highest weight has to be found in a rapidly growing search space.

A solution to ease this fast-growing set of nodes is to exploit the fact that not all nodes in the grid are of equal importance to represent the distribution of the propagation constant. Cross terms with a high total degree can be safely omitted without losing accuracy. This procedure leads to sparse grids, such as the Smolyak grid [10], used in this incarnation of ST. By applying the ST node picking algorithm on the reduced set of grid nodes, the matrix equation (6) remains well-conditioned and maintains a reasonable run-time.

III. Reduced-order Stochastic Testing

With the random realization $\boldsymbol{\xi}_i$ chosen, the FEM solver needs to be invoked for each corresponding roughness profile and the subsequent eigenvalue problem (2) has to be solved. The operation to invert this $2n \times 2n$ matrix, with n the number of basis functions on the FEM mesh, is resource intensive but can be sped-up. Each run of the full-wave simulation solves a configuration that does not differ that much from the previous one, so some information should be transferable or recyclable. To exploit this redundancy to the fullest, the approach advocated in [6] is adapted to the generalized eigenvalue problem (2). The core idea is to construct an $(2n \times m)$ orthogonal projection matrix $\overline{\overline{Q}}$ composed of m orthonormal basis vectors $\mathbf{e}_j$, with $m \ll 2n$, such that (2) can be transformed into

$$\overline{\overline{\tilde{A}}}\tilde{\mathbf{x}} = \tilde{\beta}\overline{\overline{\tilde{B}}}\tilde{\mathbf{x}}, \tag{7}$$

with $\overline{\overline{\tilde{A}}} = \overline{\overline{Q}}^T \overline{\overline{A}}\,\overline{\overline{Q}}$, $\overline{\overline{\tilde{B}}} = \overline{\overline{Q}}^T \overline{\overline{B}}\,\overline{\overline{Q}}$ and $\tilde{\beta}$ the approximated propagation constant with its eigenvector $\tilde{\mathbf{x}}$ in the subspace spanned by $\{\mathbf{e}_j\}$. With the resulting matrix equation reduced to dimension m, it can be solved in a fraction of the time, thus reducing the overall computation time.

The question of course remains how to efficiently construct $\overline{\overline{Q}}$ to obtain a considerable efficiency gain without sacrificing too much accuracy. The applied strategy consists of solving the full, non-reduced eigenvalue problem (2) for a few, well-chosen nodes of the $K+1$ realizations in $\{\boldsymbol{\xi}_j\}$ and extract their eigenvectors as a starting point for the projection matrix. In this contribution, we choose for this set, named $\{\boldsymbol{\xi}_j\}_{\text{base}}$, $N_{\text{RV}}+1$ specific elements of $\{\boldsymbol{\xi}_j\}$, namely the nominal problem and N_{RV} realizations of $\boldsymbol{\xi}_i$ along the main directions of $\boldsymbol{\xi}$. These vectors correspond to points on the sparse grid with the highest weight along the axis of each individual normal random variable. Depending on the nature of the configuration under study other choices for $\{\boldsymbol{\xi}_j\}_{\text{base}}$ might be opportune but for the analysis of rough interconnects in this contribution, the approach has proven to be very successful as will be shown in Section IV. With the starting set fixed, the algorithm for constructing $\overline{\overline{Q}}$ is as follows:

1) Solve (2) for the $N_{\text{RV}}+1$ elements of $\{\boldsymbol{\xi}_j\}_{\text{base}}$ and store their corresponding eigenvectors $\{\mathbf{x}_j\}_{\text{base}}$.
2) Initialize $\overline{\overline{Q}}$ as $\dfrac{\mathbf{x}_0}{||\mathbf{x}_0||}$ with $\mathbf{x}_0$ the eigenvector corresponding to the nominal problem.
3) For each of the remaining eigenvectors in $\{\mathbf{x}_j\}_{\text{base}}$, compute $\mathbf{x}_j^{\perp} = \mathbf{x}_j - \overline{\overline{Q}}\left[\overline{\overline{Q}}^T \mathbf{x}_j\right]$. If $||\mathbf{x}_j^{\perp}||$ is larger than a predetermined threshold value, expand the column space of $\overline{\overline{Q}}$ with $\mathbf{x}_j$, resulting in $\overline{\overline{P}} = \left[\overline{\overline{Q}} \mid \mathbf{x}_j\right]$.
4) Calculate an updated version of $\overline{\overline{Q}}$ by performing a QR-decomposition on $\overline{\overline{P}} = \overline{\overline{Q}}'\overline{\overline{R}}$ to get a numerically stable computed orthogonal projection matrix. As a last action, replace $\overline{\overline{Q}}$ by its updated successor $\overline{\overline{Q}}'$.

5) Repeat step 3) and 4) for the remaining eigenvectors in $\{\mathbf{x}_j\}_{\text{base}}$ and terminate once all eigenvectors have been tested and, if necessary, added to $\overline{\overline{Q}}$. In the end, a $(2n \times m)$ matrix has been constructed with $m \leq N_{\text{RV}} + 1$.

The remaining $K - N_{\text{RV}}$ elements of $\{\boldsymbol{\xi}_j\}$ can now be solved through (7) in the reduced space.

IV. Application to Interconnect Structures

We first apply the proposed method to the rectangular waveguide analyzed in [2], to verify the validity of the reduced-order ST and demonstrate its speed-up. Secondly, we look at a microstrip configuration to show the applicability to more widespread, realistic interconnect configurations. All calculations were performed on a machine with an Intel®core™i7-3770 CPU at a clock of 3.4 GHz with 32 GB of RAM.

A. Rough rectangular waveguide

Consider a rectangular waveguide with dimensions $2l$ and $1l$ along the x-axis and y-axis, respectively, with l an arbitrary length unit. With a wavenumber $k_0 = 10l^{-1}$, a discretization of 1094 triangles is required, leading to a total of 5745 unknowns, in a second-order FEM expansion. Roughness is simulated by displacing 82 edge nodes along the rectangle's boundary. The constants defining the roughness profile are $\sigma_r = 0.01l$ and $L_c = 0.5l$ which leads to $N_{\text{RV}} = 8$ after a KLT with $\Theta = 0.85$. Therefore, the set $\{\xi_j\}_{\text{base}}$ contains 9 realizations that are solved in the full space. For a PCE with maximal order of expansion $P_{\text{max}} = 2$, the total number of polynomials, and thus also of required realizations, is given by $K+1 = 45$ (see (5)). Hence, the remaining $45-9 = 36$ nodes can now be calculated in the reduced space.

Comparing the distribution of the propagation constant of the lower-order, i.e., the TE_{10} mode, with a Monte Carlo approach of 50000 samples, we obtain the correspondence shown in Figure 2. The curve of the reduced-order ST was obtained by performing a MC analysis on the polynomial model (4), which owing to the ease of evaluation of such a model took a mere fraction of the brute force MC method. The average and standard deviation of β are tabulated in Table I together with those of the MC, ST and SPCE [2] methods. The obtained standard deviation is slightly higher than the other methods predict but this can be attributed to a small loss of accuracy by projecting on the reduced solution space. A Cramér-von Mises test [11] on both distributions in Fig. 2 yields in a p-value of 0.149, confirming that both sets of results stem from the same distribution.

The main goal of the reduced-order ST was to reduce the calculation time without significantly sacrificing accuracy. Having confirmed the latter, we turn to the former. From Table II, we clearly see a speed-up of about a factor four obtained on the total calculation time. The breakdown of the computation time over the various steps in the algorithms exposes the origin of this speed-up: the computation of the eigenvectors in the full space is such a dominant contribution

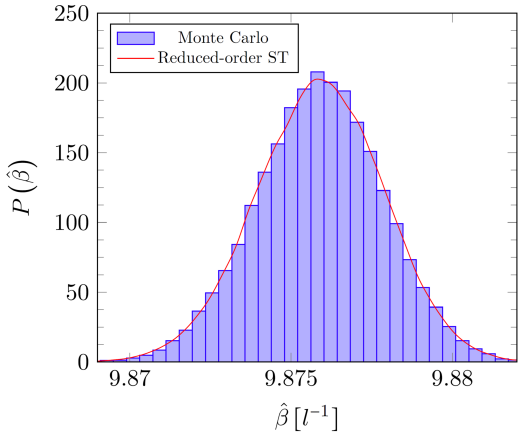

Fig. 2. Distribution comparison of the TE_{10} mode propagation constant for a rectangular waveguide by a Monte Carlo approach and a reduced-order ST technique.

TABLE I
STATISTICS OF THE TE_{10} PROPAGATION CONSTANT OBTAINED BY MC, SPARSE ST, SPC AND REDUCED-ORDER ST

Method	$\mu\ [l^{-1}]$	$\sigma\ [l^{-1}]$
MC	9.87589	0.00192
ST [2]	9.87590	0.00196
SPCE [2]	9.87589	0.00196
Reduced-Order ST	9.87588	0.00197

to the run-time that the, albeit rather limited, overhead of the arithmetic involved in constructing the $\overline{\overline{Q}}$-matrix is immediately compensated by a reduced number of large matrix solutions.

B. Microstrip interconnect

Our second example constitutes a microstrip interconnect on a (lossless) RO4003C substrate bounded by a perfect electric conductor (PEC) box. The cross-section is meshed with 3333 triangles, with a finer discretization near the metallic strip in anticipation of strong fringing fields in this region. Subjecting the 154 nodes on the central strip to LER, the distribution on their deviation is governed by $\sigma_r = 1\,\mu\text{m}$ and $L_c = 0.1\,\text{mm}$ which leads to $N_{\text{RV}} = 13$ after a KLT with $\Theta = 0.85$. Given a second-order PCE, this leads to $K + 1 = 105$ runs, in correspondence with (5), of the FEM

TABLE II
COMPARISON OF THE CALCULATION TIME BETWEEN THE ST [2] AND THE REDUCED-ORDER ST METHODS. t_{EIG} IS THE CALCULATION TIME TO SOLVE (2), t_{RED} THE TIME TO SOLVE (7), t_{Q} THE CALCULATION TIME FOR CONSTRUCTING $\overline{\overline{Q}}$ AND t_{TOT} THE TOTAL COMPUTATION TIME.

Waveguide	t_{eig} [s]	t_{red} [s]	t_{Q} [s]	t_{tot} [s]
ST	$45 \cdot 1.97$	/	/	88.8
Reduced-Order ST	$9 \cdot 1.97$	$36 \cdot 0.0857$	0.37	21.2
Microstrip	t_{eig} [s]	t_{red} [s]	t_{Q} [s]	t_{tot} [s]
ST	$105 \cdot 8.81$	/	/	925.05
Reduced-Order ST	$14 \cdot 8.81$	$91 \cdot 0.0588$	2.66	131.35

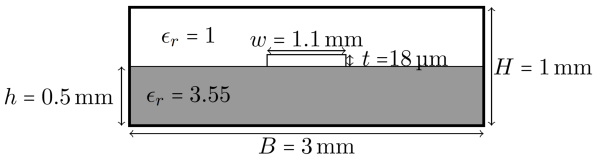

Fig. 3. Schematic overview of the simulated microstrip interconnect with annotated dimensions and relevant material properties. The strip and boundary box are perfect electric conductors (PEC) with the strip subjected to roughness.

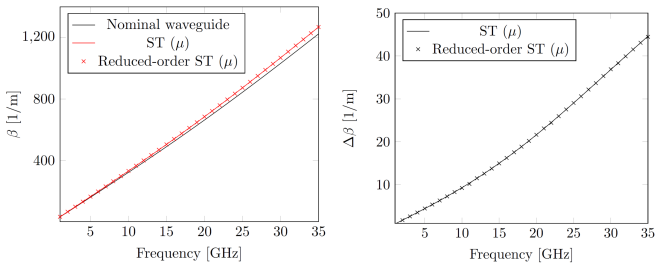

(a) β with smooth (black) and rough (red) edge.

(b) Average deviation $\Delta\beta$.

Fig. 4. Comparison of the lowest-order propagation constant as a function of the frequency, for the nominal microstrip and the average lowest-order propagation constant for a rough microstrip. a) Average β for both ST and reduced-order ST vs. a smooth microstrip. b) Average deviation $\Delta\beta$ from the nominal β as a function of frequency.

solver for every frequency point whose we would like to examine the propagation constant.

The results of this frequency sweep are given in Fig. 4a and Fig. 4b. Figure 4a compares the nominal lowest-order propagation constant to the average β for the configuration with a rough metal strip. For the rough microstrip, the results obtained by means of standard and reduced-order ST are both displayed. A very good agreement between both techniques is observed. Furthermore, it is also clearly visible that the lowest-order propagation constant tends to shift upwards as a consequence of LER. These observations are further clarified in Fig. 4b, where the nominal value of the propagation constant is subtracted from the average, again for both techniques.

The calculation time involved in solving the eigenvalue problem for one frequency sample is included in Table II. The speed-up obtained by projecting the matrix equation on a reduced space has increased to a factor of seven as compared to the rectangular waveguide due to a higher number of random variables. This further demonstrates that the reduced-order ST is a powerful extension of the ST algorithm and augments its applicability to problems involving a ever-growing number of unknowns.

V. Conclusion

The goal of this contribution was to facilitate the analysis of line edge roughness' influence on the propagation characteristics of interconnect structures. Given the long runtime of a full-wave simulation, an order reduction technique was applied to a sparse stochastic testing method. This cuts down not only the number of calls required to the full-wave solver but also drastically reduces the solution time of the generalized eigenvalue problem required to extract the propagation constant in the lion's share of the runs required to characterize the probability distribution. The framework was successfully applied to a rough rectangular waveguide and a rough microstrip interconnect.

References

[1] H. Gao, S. De and S. Payne, "Impact of Surface Roughness on Return Planes in High Speed Signal Propagation". *2020 IEEE International Symposium on Electromagnetic Compatibility & Signal/Power Integrity (EMCSI)*, Reno, NV, USA, 2020, pp. 150-154.

[2] R. Waeytens, D. Bosman, M. Huynen, M. Gossye, H. Rogier and D. Vande Ginste, "Analysis of the Influence of Roughness on the Propagation Constant of a Waveguide via Two Sparse Stochastic Methods". *2020 IEEE 29th Conference on Electrical Performance of Electronic Packaging and Systems (EPEPS)*, San Jose, CA, USA, 2020, pp. 1-3.

[3] G. Blatman and B. Sudret, "An adaptive algorithm to build up sparse polynomial chaos expansions for stochastic finite element analysis". *Probabilistic Engineering Mechanics*, vol. 25, 2009, pp. 183–197.

[4] Z. Zhang, T. A. El-Moselhy, I. M. Elfadel, and L. Daniel,"Stochastic testing method for transistor-level uncertainty quantification based on generalized polynomial chaos". *IEEE Transactions on Computer-Aided Design of Integrated Circuits and Systems*, vol. 32, no. 10, 2013, pp. 1533– 1545.

[5] M. Gossye, G. Gordebeke, K. Y. Kapusuz, D. Vande Ginste, and H. Rogier, "Uncertainty quantification of waveguide dispersion using sparse grid stochastic testing". *IEEE Transactions on Microwave Theory and Techniques*, vol. 68, no. 7, 2020, pp. 2485–2494.

[6] T. El-Moselhy and L. Daniel, "Variation-aware interconnect extraction using statistical moment preserving model order reduction". *Design, Automation & Test in Europe Conference & Exhibition*, Dresden, Germany, 2010, pp. 453-458.

[7] R. D. Graglia, A. F. Peterson and F. P. Andriulli, "Curl-conforming hierarchical vector bases for triangles and tetrahedra". *IEEE Transactions on Antennas and Propagation*, vol. 59, no. 3, 2011, pp. 950-959.

[8] Z. Zubac, D. De Zutter and D. Vande Ginste, "Scattering From Two-Dimensional Objects of Varying Shape Combining the Method of Moments With the Stochastic Galerkin Method". *IEEE Transactions on Antennas and Propagation*, vol. 62, no. 9, 2014, pp. 4852-4856.

[9] Z. Zubac, L. Daniel, D. De Zutter and D. Vande Ginste, "A Cholesky-Based SGM-MLFMM for Stochastic Full-Wave Problems Described by Correlated Random Variables". *IEEE Antennas and Wireless Propagation Letters*, vol. 16, 2017, pp. 776-779.

[10] F. Heiss and V. Winschel, "Likelihood approximation by numerical integration on sparse grids". *Journal of Econometrics*, vol. 144, no. 1, 2008, pp. 62-80.

[11] T. W. Anderson, "On the Distribution of the Two-Sample Cramér-von Mises Criterion". *Ann. Math. Statist.*, vol. 33, 1962, pp. 1148–1159.